

RESEARCH PAPER



Engineering non-pathogenic bacteria for auto-transporter-driven secretion of functional interferon

May Tfilin Samuel, Irina Rostovsky, Alona Kuzmina, Ran Taube , and Neta Sal-Man 

The Shrager Segal Department of Microbiology, Immunology, and Genetics, Faculty of Health Sciences, Ben-Gurion University of the Negev, Beer-Sheva, Israel

ABSTRACT

In recent years, various strategies have been developed to enable the oral administration of protein-based drugs (biologics) with the aim of overcoming the degradation and inactivation of these drugs that can occur as they traverse the gastrointestinal tract (GIT). In this study, we investigated bacteria as a delivery vehicle for biologics, harnessing their ability to withstand the harsh gastric environment and deliver therapeutic drugs directly to the intestine. Specifically, we explored using the type 5 secretion system (T5SS) to secrete therapeutic cargoes under simulated gut conditions. Our research focused on EspC, a T5SS protein from enteropathogenic *Escherichia coli*, and its potential to secrete interferon- α (IFN α), a cytokine with immunomodulatory and antiviral properties widely used in the clinic. We demonstrated that EspC can facilitate the secretion of IFN α variant when expressed in nonpathogenic bacteria. Moreover, this EspC-secreted IFN was able to activate the JAK-STAT pathway, upregulate IFN-stimulated genes, and induce a robust antiviral response in cells. Collectively, these findings provide proof of concept supporting the utilization of the EspC protein as a novel delivery platform for protein-based therapeutics.

ARTICLE HISTORY

Received 25 November 2024
Revised 30 January 2025
Accepted 25 February 2025

KEYWORDS

Antiviral; EspC; Interferon; oral drug delivery; protein secretion; type V secretion system



Introduction


Protein and peptide-based drugs (biologics) have emerged as a promising class of therapeutic agents due to their high selectivity, efficacy, and reduced side effects compared to small molecule drugs. The oral delivery of biologics, as well as other drugs, is usually favored over parenteral administration due to ease of administration, improved patient compliance, and reduced production costs. However, the oral administration of biologics is challenging due to the enzymatic and chemical/physical degradation of these drugs in the gastrointestinal tract (GIT).^{1,2}

Several strategies have been developed to address the challenges associated with the oral administration of biologics, including chemical modifications such as PEGylation and pro-drug designs, nanoparticle-based delivery systems, and the co-administration of protease inhibitors and absorption-enhancing compounds alongside the therapeutic protein.¹ However, these approaches

often reduce the efficiency of these biologics and are associated with high production costs.^{1,3} Engineered bacteria have emerged as promising platforms for the oral delivery of therapeutic proteins and peptides. Recent studies have demonstrated the feasibility of utilizing these bacteria to express and secrete therapeutic molecules directly in the gastrointestinal tract.^{4,5} These bacteria are naturally designed to withstand the harsh conditions found in the stomach, allowing them to reach the small intestine and colon, where they can release the therapeutic proteins without the need for complex purification processes.⁶

Bacterial secretion systems present a promising option for engineering bacteria to secrete therapeutic proteins.⁷ Bacteria normally use these secretion systems to transport proteins across their cell membranes, and they play crucial roles in bacterial physiology, pathogenesis, and interactions with the environment.^{6,8} A prominent example of a bacterial secretion system previously utilized for

CONTACT Neta Sal-Man  salmanne@bgu.ac.il  The Shrager Segal Department of Microbiology, Immunology, and Genetics, Faculty of Health Sciences, Ben-Gurion University of the Negev, Beer-Sheva 84105, Israel

 Supplemental data for this article can be accessed online at <https://doi.org/10.1080/19490976.2025.2474146>

© 2025 The Author(s). Published with license by Taylor & Francis Group, LLC.

This is an Open Access article distributed under the terms of the Creative Commons Attribution-NonCommercial License (<http://creativecommons.org/licenses/by-nc/4.0/>), which permits unrestricted non-commercial use, distribution, and reproduction in any medium, provided the original work is properly cited. The terms on which this article has been published allow the posting of the Accepted Manuscript in a repository by the author(s) or with their consent.

biologics delivery is the type 3 secretion system (T3SS).^{9–11} This secretion system, found in many Gram-negative pathogens, is a syringe-like apparatus comprising more than 20 different proteins that can inject effector proteins across the bacterial outer membrane and into host cells.^{12–15} The T3SS has been shown to mediate the secretion of recombinant proteins such as vaccine antigens, enzymes, transcription factors, and anticancer drugs.^{6,16} Our group previously demonstrated that we can utilize the T3SS of enteropathogenic *Escherichia coli* (EPEC) to secrete functional interferon- α 2 (IFN α 2) across the bacterial outer membrane and into the extracellular environment.¹⁷ While the T3SS is an exciting secretion system that has been shown to promote the secretion of various proteins,^{9–11} the complex is expressed mainly in pathogenic bacteria. While several groups have successfully transferred the T3SS into nonpathogenic strains,¹⁸ safety concerns persist.

In light of these issues, we attempted to use the type V secretion system (T5SS) as an alternative secretion system. The T5SS, also known as the autotransporter system, represents one of the most widespread protein secretion pathways in Gram-negative bacteria. This system is responsible for secreting an extensive variety of proteins, including enzymes and toxins.^{19–25} Autotransporters encode all the necessary components for their own secretion within a single protein and can be divided into several sub-groups, according to their domain arrangement and functional properties.²⁶ T5SS includes an N-terminal signal peptide (SP), which is recognized by the Sec-mechanism and facilitates protein translocation across the inner membrane. In addition, they have a passenger domain (PD), which is the secreted portion of the protein, and a C-terminal translocator domain that forms a β -barrel pore across the outer membrane^{23,27} (Figure 1). Another key autotransporter component is a short linker domain positioned between the PD and the β -barrel domain, which includes an α -helix and a disordered region that facilitates the passage of the PD through the β -barrel domain.^{28,29} It has also been demonstrated that T5SS-mediated PD secretion requires the interaction between the β -barrel domain and the BamA protein, which creates the lumen through which the PD passes.^{30,31}

Since PD secretion is accomplished by a single protein together with the general bacterial secretory machinery, such as the Sec and Bam complexes, it offers a straightforward method for introducing the T5SS into nonpathogenic bacteria. However, the T5SS may face limitations in its ability to secrete proteins that contain disulfide bonds or require certain post-translational modifications.³² These features could interfere with the translocation process or necessitate additional engineering to maintain the desired protein conformation.^{33,34}

Here, we sought to study whether EspC, a T5SS protein expressed in EPEC, can be used as a delivery system. EspC is a 110 kDa serine protease autotransporter that belongs to the serine protease autotransporters of Enterobacteriaceae (SPATE) subfamily.^{34,35} EspC, like many other autotransporters, is initially translocated into the periplasm via a Sec-dependent mechanism. During this process, the SP is cleaved, and the C-terminal β -barrel forms a pore in the outer membrane. This pore interacts with BamA to facilitate the transport of the PD across the membrane,³⁰ where it is ultimately released into the external environment through cleavage in the linker domain (Figure 1(a)). The PD release is executed through a proteolytic cleavage at the linker region, specifically between two conserved adjacent asparagine residues, separating it from the membrane-embedded β -barrel domain.^{36–38} The SPATE proteins exhibit serine protease activity, leading to the initial hypothesis that they autonomously catalyze the C-terminal cleavage. However, experimental evidence demonstrates that disrupting or deleting the serine endopeptidase within the PD retains the ability to detach from the β -barrel component.³⁴ This indicates that this process is independent of the serine protease domain and is likely mediated by the cyclization of the conserved asparagine residues.^{36–38}

In this study, we examined whether EspC can be employed to secrete a type I IFN (IFN). IFNs are a family of cytokines that play crucial roles in innate antiviral immunity, the modulation of adaptive immunity, and the induction of antiproliferative effects.³⁹ All type I IFNs bind to a common cell surface receptor composed of two subunits, IFNAR1 and IFNAR2, which activates the JAK-

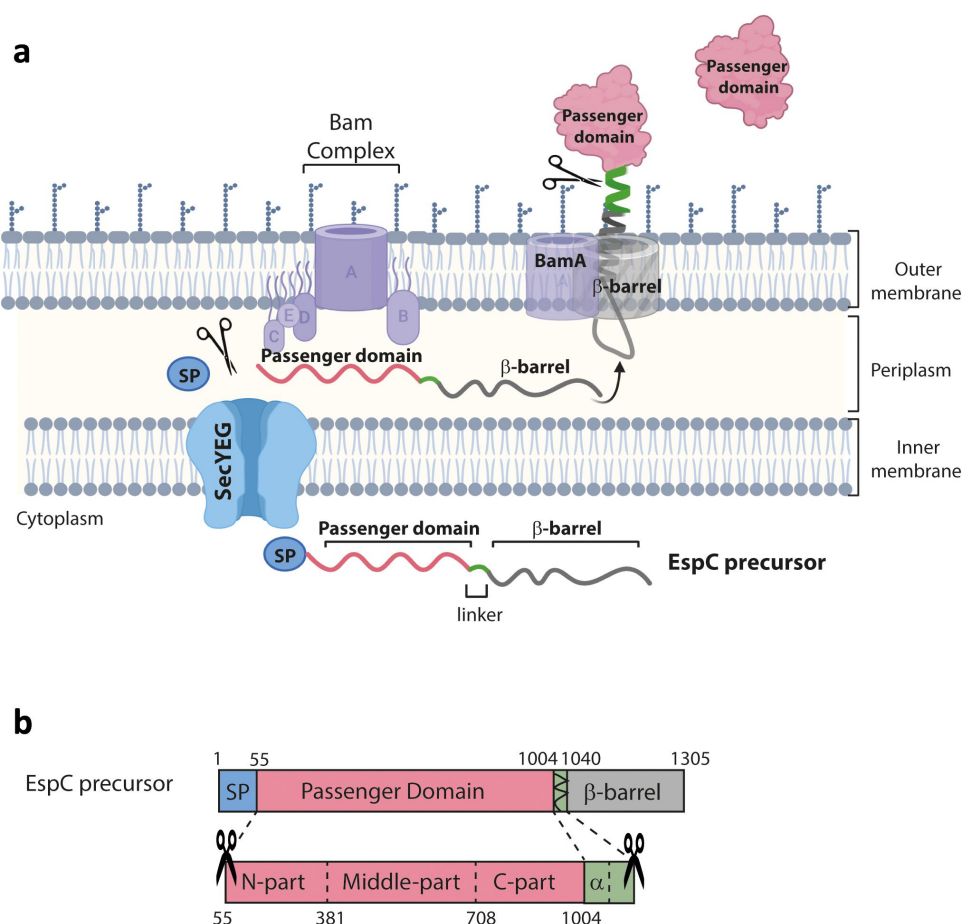


Figure 1. Schematic representation of EspC secretion pathway and domain organization. (a) The EspC precursor protein is first recognized by the Sec machinery (embedded within the inner membrane and indicated in blue) through its N-terminal signal peptide (SP; light blue) and then transported into the periplasmic space, where the SP is cleaved. The β -barrel domain (gray) folds across the outer membrane and interacts with the Bam complex (light purple) to allow the passenger domain (pink) to pass through the pore and reach the bacterial surface. The passenger domain is then cleaved off (at the linker sequence – green) and released into the extracellular medium. (b) Schematic diagram of the EspC precursor. The protein contains an N-terminal signal peptide (SP; light blue), a passenger domain (pink), which is the secreted portion, a linker region (green) that contains an α -helix and a cleavage site, and the β -barrel domain (gray). The three sections of the passenger domain utilized in this study are shown.

STAT signaling pathway, leading to the upregulation of numerous interferon-stimulated genes (ISGs) that modulate the immune response.^{39–41} Among these type I IFNs, IFN α 2 and IFN β have been widely used in the clinic for the treatment of chronic viral infections such as hepatitis B, as well as various cancers including hairy cell leukemia, malignant melanoma, and AIDS-related Kaposi's sarcoma.^{42,43} Type I IFNs are an attractive therapeutic agent, given their numerous roles in regulating the immune response. Their administration typically entails a regimen that involves frequent intramuscular or subcutaneous injections, reducing patient compliance.

The T5SS has been extensively studied as a mechanism for protein display and secretion, with

research predominantly focusing on two key applications; the presentation and secretion of bacterial antigens for vaccine development^{19,44} and displaying human proteins for large-scale pharmaceutical production.^{45–47} However, its potential as a direct platform for secreting biologically active human proteins for therapeutic purposes remains largely unexplored. Here, we examined the ability of a highly potent version of IFN α 2, containing three mutations along the protein sequence (H57Y, E58N, Q61S – referred to as YNS), to be secreted using the EspC protein. This YNS version elicited an enhanced signal transduction response, as demonstrated by its 60-fold and 3-fold greater binding affinity for IFNAR1 compared to wildtype IFN α 2 and IFN β , respectively. The YNS mutations generate an 'IFN β -like' version of

IFN α 2, thus rendering it more therapeutically potent.⁴³ In this study, we found that IFN α 2 can be secreted via the EspC autotransporter when expressed in nonpathogenic bacteria. Overall, our results provide a proof of concept that the EspC protein can be employed as a novel delivery system for protein-based drugs.

Materials and methods

Bacterial strains

Wildtype (WT) enteropathogenic *Escherichia coli* (EPEC) O127:H6 strain E2348/69, EPEC Δ espC mutant, which lacks the native EPEC T5SS EspC protein, and EPEC Δ lee mutant, which includes the deletion of the entire locus of enterocyte effacement (LEE), were used to examine the expression and secretion of the various EspC proteins (Table 1). WT TOP10 *E. coli* and TOP10 *E. coli* Δ dsbA mutant, in which the protein that catalyzes disulfide bond formation in *E. coli* was deleted, were used to evaluate the T5SS activity of EspC in nonpathogenic strains (Table 1).

Construction of EspC expression vectors

To identify EspC domains that are non-essential for its autosecretory function, we generated two EspC versions: EspC_{N+C}, which lacks the middle portion of the passenger domain (PD), and EspC_C, which lacks both the N-terminus and the middle parts of the PD (Figure 2). To do so, we first

amplified the full-length *espC* gene from EPEC genomic DNA using the primer pair EspC_F/EspC_R (Table 2). In parallel, the pSA10 vector was amplified using the primer pair vector_F/vector_R (Table 2). The open plasmid and the fused PCR product were treated with *DpnI*, purified, and assembled using the Gibson assembly method^{53,54} to create the pEspC vector. To create the pEspC_{N+C} construct, we amplified the pEspC vector using the primer pair N+C_vector_F/N+C_vector_R (Table 2). Those primers amplified the plasmid, including the pEspC signal sequence, the C-part of the passenger domain, and the β -barrel domain. In parallel, we amplified the N-terminal part of the EspC passenger domain using the primer pair N+C_insert_F/N+C_insert_R (Table 2), which fused a Flag tag at the N-terminus of the PCR fragment. The open plasmid and the PCR fragment were treated with *DpnI*, purified, and assembled using the Gibson assembly method to create the pEspC_{N+C} vector. To construct the pEspC_C plasmid, we amplified the pEspC_{N+C} using the primer pair C_vector_F/C_vector_R (Table 2). The vector was then treated with *DpnI*, purified, and self-assembled in a Gibson assembly reaction to create the pEspC_C vector. To construct the pEspC+IFN plasmid, we amplified the pEspC vector using the primer pair IFN_vector_F/IFN_vector_R (Table 2), and the IFN_{YNS} encoding sequence from the pT7T318U plasmid (Table 1) using the primer pair IFN_insert_F/IFN_insert_R (Table 2). The open plasmid and the PCR fragment were treated with

Table 1. Strains and plasmids used in this study.

Strain/Plasmid	Description	Reference
Strains		
WT EPEC	EPEC strain E2348/69, streptomycin-resistant	48
EPEC Δ espC	Genomic deletion of <i>espC</i> , streptomycin-resistant	This study
EPEC Δ lee	Genomic deletion of the locus of enterocyte effacement (LEE), streptomycin-resistant	49
<i>E. coli</i> TOP10	<i>E. coli</i> K12 F ⁻ mcrA Δ (mrr-hsdRMS-mcrBC) ϕ 80lacZAM15 Δ lacX74 <i>recA1</i> <i>araD139</i> Δ (<i>ara-leu</i>)7697 <i>galU</i> <i>galK</i> λ - <i>rpsL</i> (Str ^R) <i>endA1</i> <i>nupG</i> . Streptomycin-resistant	Thermo Fisher
<i>E. coli</i> TOP10 Δ dsbA	<i>E. coli</i> K12 F ⁻ mcrA Δ (mrr-hsdRMS-mcrBC) ϕ 80lacZAM15 Δ lacX74 <i>recA1</i> <i>araD139</i> Δ (<i>ara-leu</i>)7697 <i>galU</i> <i>galK</i> λ - <i>rpsL</i> (Str ^R) <i>endA1</i> <i>nupG</i> Δ dsbA. Streptomycin-resistant	50
Plasmids		
pT7T318U	Cloned human IFN α 2 gene with YNS mutations.	43
pRE112	Suicide vector for allelic exchange, chloramphenicol resistance.	51
pEspC (pSA10)	Full-length EspC encoding sequence within the pSA10 vector.	This study
pEspC _{N+C}	EspC SP, N- and C parts of the PD, and the β -barrel domains encoded on the pSA10 plasmid, carbenicillin resistant.	This study
pEspC _C	EspC SP, C-part of the PD, and the β -barrel domains encoded on the pSA10 plasmid, carbenicillin resistant.	This study
pEspC+IFN	Human IFN α 2 gene encoded between the EspC SP and the β -barrel domains. pSA10 plasmid, carbenicillin resistant.	This study
pEspC _C +IFN	Human IFN α 2 gene encoded between the EspC SP and the C-part of the PD and the β -barrel domains. pSA10 plasmid, carbenicillin resistant.	This study
pEspC _{del}	pRE112 containing the flanking regions of <i>espC</i> , chloramphenicol resistance.	This study
pHR-CMV-GFP	GFP-expressing lentivirus	52

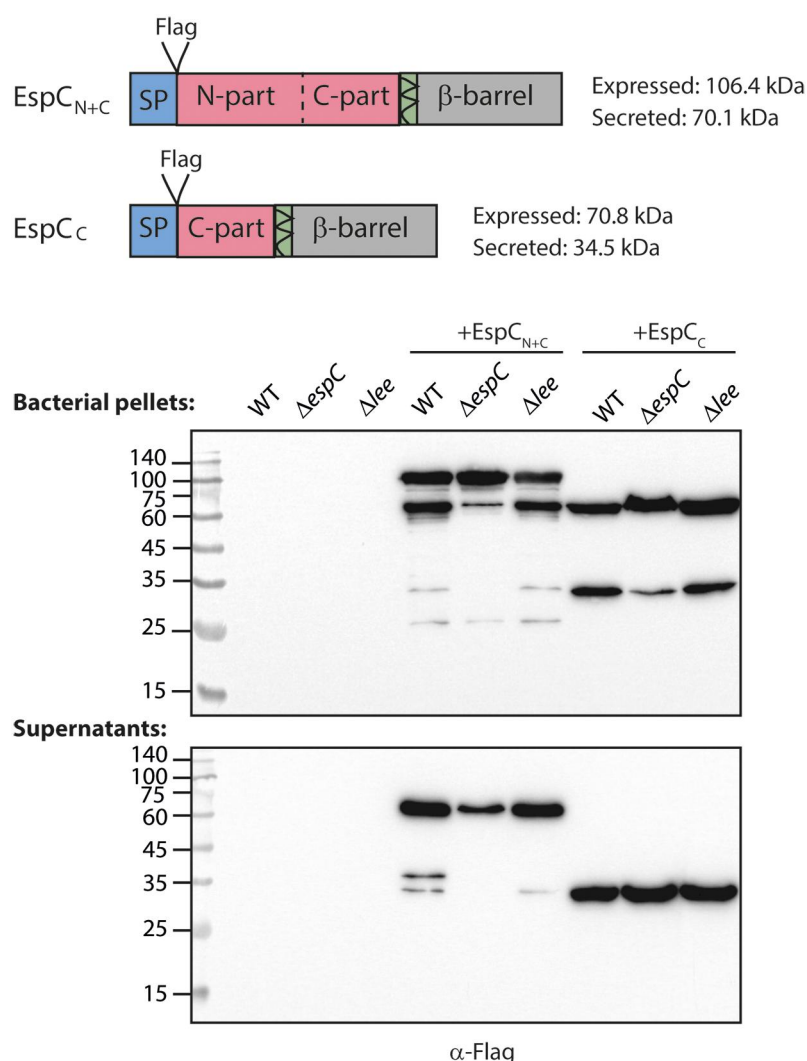


Figure 2. The EspC_C construct supports type 5 secretion. Domain organization of the truncated EspC protein versions (EspC_{N+C} and EspC_C) and their expected sizes (expressed precursors and the secreted versions) are presented. The constructs were transformed into EPEC wildtype (WT), $\Delta espC$ (deletion of the *epsC* gene), and Δlee (deletion of the entire LEE pathogenicity island) strains and grown under T3SS-simulating conditions for 6 h. The cultures were then centrifuged to separate the supernatants (secreted fraction) from the bacterial pellets. The volumes of supernatants were normalized according to OD₆₀₀ values, concentrated, and analyzed along with the bacterial pellets via SDS-PAGE and western blotting with an anti-flag antibody. The expression (upper panel, bacterial pellets) and EspC-mediated secretion (lower panel, supernatants) demonstrate that the truncated EspC versions are expressed and secreted.

DpnI, purified, and assembled using the Gibson assembly method to create the pEspC+IFN vector. To create the pEspC_C+IFN vector, we amplified the pEspC_C vector using the primer pair C_vector_F/IFN_C_vector_R (Table 2), and the IFN_{YNS} coding sequence from the pT7T318U plasmid (Table 1), using the primer pair IFN_insert_F1/IFN_insert_R1 (Table 2). The PCR fragment was then re-amplified using primer pair IFN_insert_F1/IFN_insert_R2 (Table 2). The plasmid and the final PCR fragment were treated with *DpnI*, purified, and assembled using the Gibson assembly method to create the pEspC_C+IFN vector.

All constructs were verified by DNA sequencing and are listed in Table 1.

Construction of the null $\Delta espC$ EPEC mutant strain

The nonpolar deletion of *espC* in the WT EPEC O127:H6 strain E2348/69 was generated using the *sacB*-based allelic exchange method.⁵¹ Briefly, PCR fragments of the flanking upstream and downstream regions of *espC* (0.9 and 1.32 kb, from the 5' and 3' ends of *espC*, respectively) were amplified from the EPEC genome with the corresponding primer pairs EspC_{up}_F/EspC_{up}_R and

Table 2. Sequences of primers used in this study.

Construct/gene	Primer name	Sequence
pEspC (pSA10)	EspC_F	CACACAGGAAACAGATGAATAAAATATACGCATTAAATATTGTCAC
	EspC_R	GATCCCCGGGAATTCAGAAAGAATAACGGAAGTTAGC
	Vector_F	AATTCCTGGGATCCGTCG
	Vector_R	CTGTTTCCTGTGAAATTGTTATCCG
pEspC _{N+C} (pSA10)	N+C_vector_F	AATCACTCATTACTGGATATTGG
	N+C_vector_R	GTCGTCATCGTCTTTGTAGTCAGCAGCCTGAGATGC
	N+C_insert_F	ACAAAGACGATGACGACAAGCTAAATATTGATAATGTATGGGCTAG
	N+C_insert_R	CCAATATCCAGTAATGAGTGATTCTTGAATGTTTATTATTACAGTG
pEspC _C (pSA10)	C_vector_F	AATCACTCATTACTGGATATTGGTAATAAAATTTACC
	C_vector_R	AGTAATGAGTGATTCTTGTGTCATCGTCTTTGTAGT
pEspC+IFN (pSA10)	IFN_vector_F	CTGATGCCGGTGCCTCG
	IFN_vector_R	TTGAGCAGCCTGAGATGCG
	IFN_insert_F	CATCTCAGGCTGCTCAAATGTGTGATCTGCCG
	IFN_insert_R	GGCACCGCATCAGATTCTTACTTCTTAACTTTCTTGC
pEspC _C +IFN (pSA10)	C_vector_F	AATCACTCATTACTGGATATTGGTAATAAAATTTACC
	IFN_C_vector_R	CTTGTGTCATCGTCTTTGTAGTC
	IFN_insert_F1	CTACAAAGACGATGACGACAAGATGTGTGATCTGCCGACG
	IFN_C_insert_R1	GTAATGAGTGATTTTCTTACTTCTTAACTTTCTTGC
pEspC _{del} (pRE112)	IFN_C_insert_R2	TTACCAATATCCAGTAATGAGTGATTTTCTTACTTC
	EspC _{up} _F	CGCGCGAGCCCCGCGCGAGCCGGG
	EspC _{up} _R	CAAGCTTCTTAGAGGTACCGGCGTTTTCGCAACCAAGTGAACGGTCAC
	EspC _{down} _F	GAGCTCGATATCGCATGCCCTTCTGCGGTAAGCCCCCTG
	EspC _{down} _R	GCTCGCGCGGGGCTGCCGCGAGCGG
	pRE112_F	GCATGCGATATCGAGCTC
	pRE112_R	GGTACCTCTAGAAGAAGCTTG
	ACTIN	TCCATCATGAAGTGTGACGT
OAS2	Actin_F	CTCAGGAGGAGGAATGATCT
	Actin_R	AAGTCAGCTTTGAGCCTCCC
MX2	OAS_F	CCAGAACTCAGCTGACCCAG
	OAS_R	TTTAAACCCTCTGCGGACGC
PKR	MX_F	TAGCGGTCTCACTCTGCTCT
	MX_R	TCTTCGCTGGTATCACTCGTC
	PKR_F	TTCTCCCGTATCCTGGTTGG
	PKR_R	

EspC_{down}_F/EspC_{down}_R (Table 2). The fragments were then annealed to each other using the primer pair EspC_{up}_R/EspC_{down}_F (Table 2) in an overlap extension PCR reaction. In parallel, the pRE112 suicide vector was linearized by PCR using the pRE112_F/pRE112_R primer pair (Table 2). The linearized pRE112 plasmid and the annealed PCR product were treated with *DpnI*, purified, and assembled using the Gibson assembly method.^{53,54} The resulting pEspC_{del} plasmid (Table 1) contained the flanking regions of *espC*, with 91% of *espC* having been deleted. The plasmid was then transformed into the *E. coli* SM10λpir conjugative strain to be introduced into WT EPEC. After a sucrose selection process, EPEC colonies susceptible to chloramphenicol were screened for the deletion of *espC* by PCR. The deletion of the *espC* gene was confirmed by sequencing.

Type 5 secretion assay

To evaluate protein secretion through the T5SS, bacteria (EPEC and TOP10 *E. coli* strains) were

initially grown overnight in LB medium supplemented with selective antibiotics in a shaker at 37°C. The overnight cultures were then diluted into pre-heated DMEM media and grown statically for 6 h in a tissue culture incubator with 5% CO₂. To examine secretion under culture conditions simulating gut, overnight cultures were grown in synthetic fecal stool media (Biochemazone). This artificial media contains amino acids, uric acid, urea, lactic acid, ammonia, creatinine, sodium, calcium, potassium, zinc, iron, sulfate, chloride, magnesium, citrate, carbonate, cellulose, yeast, gelatin, oleic acid, glycerol, and acetic acid. The cultures were grown for 6 h in an anaerobic chamber (Whitley A35 anaerobic workstation with 10% CO₂, 5% H₂, and 85% N₂). Due to the high density of the synthetic fecal stool media, we mixed it with DMEM at three dilution levels (1:1, 1:5, and 1:10). Protein expression in strains containing the pSA10 vectors was induced by adding 0.1 mM IPTG to bacterial cultures following a 2-hour incubation. The cultures were then centrifuged for 5 min at 1,500 × g to separate bacterial pellets from culture

supernatants. The pellets were resuspended in SDS-PAGE sample buffer, while the supernatants, containing the secreted proteins, were filtered through a 0.22- μ m filter (Millipore). The volumes of the supernatants were normalized based on the bacterial OD₆₀₀ values and treated with 10% (v/v) trichloroacetic acid (TCA) overnight at 4°C to precipitate the proteins. Following precipitation, samples were centrifuged at 18,000 \times g for 30 min at 4°C. The resulting protein precipitates were dissolved in SDS-PAGE sample buffer, and any remaining TCA in the samples was neutralized using saturated Tris. Bacterial pellets and supernatants were analyzed for protein expression and secretion, respectively, via SDS-PAGE and western blotting. To assess bacterial growth in cultures containing synthetic fecal material, samples were collected at the end of the growth period, serially diluted in sterile PBS, plated on LB agar supplemented with carbenicillin, and incubated overnight in 37°C. Bacterial growth was quantified by counting colony-forming units (CFUs).

Western blotting

For protein detection, samples were first resolved by SDS-PAGE and then transferred onto nitrocellulose membrane (pore size: 0.45 μ m; Cytiva Protran). To reduce nonspecific antibody binding, the blots were first incubated in a blocking solution (5% (w/v) skim milk in 0.1% Tween in phosphate-buffered saline [PBST]) for 60 min. Then, the blots were incubated with the primary antibody (diluted in blocking solution) for 60 min at room temperature or overnight at 4°C, washed with PBST, and incubated with horseradish peroxidase (HRP)-conjugated secondary antibody (diluted in blocking solution) for 60 min at room temperature. The blots were incubated with ECL reagents (Cyanagen) to detect chemiluminescence (BioRad). The primary antibodies included: mouse anti-Flag (Sigma) diluted 1:1,000; rabbit anti-phosphorylated STAT2 (Abcam Inc.), diluted 1:600; rabbit anti-IFN α 2 (Abcam inc.), diluted 1:1000; mouse anti-DnaK (Abcam, Inc.), diluted 1:5,000, and mouse anti-Actin (MP biomedical), diluted 1:10,000. The secondary antibodies were: HRP-goat anti-

mouse and HRP-goat anti-rabbit (Abcam Inc.), diluted 1:10,000. Western blots representative of at least three independent experiments are presented in the Results section.

Quantification of secreted IFN levels

Filtered supernatants from TOP10 *E. coli* Δ *dsbA* bacteria expressing either EspC_C or EspC_C+IFN were analyzed in triplicate using a commercial Human Interferon alpha 2 ELISA kit (Abcam Inc.). The quantification procedure followed the manufacturer's guidelines, with calibration performed against a standardized recombinant human IFN α 2 protein.

STAT2 phosphorylation assay

HT-29 and Caco-2 cells at 70% confluence were incubated with filtered supernatant samples from TOP10 *E. coli* Δ *dsbA* expressing EspC_C, EspC_C+IFN, or EspC+IFN for 1 h in a tissue culture incubator (37°C, 5% CO₂). The cells were then washed and lysed, and their protein extracts were subjected to SDS-PAGE and western blotting analyses using antibodies against phosphorylated STAT2 and actin (loading control). Recombinant IFN β (2 nM) was used as a positive control, while untreated cells were used as a negative control. For the neutralization assay, supernatant samples from TOP10 *E. coli* Δ *dsbA* expressing the EspC_C+IFN protein and samples of recombinant IFN α 2 (0.5 nM, Abcam Inc.) were left untreated or mixed with the neutralizing anti-human IFN α 2 antibody (R&D Systems) at a tenfold molar excess (5 nM) for 1 h at room temperature. The samples were then added to 70% confluent Caco-2 cells for 1 h at 37°C. The cells were then washed and lysed, and their protein extracts were subjected to SDS-PAGE and western blot analyses using antibodies against phosphorylated STAT2 and actin (loading control). The concentration of EspC_C+IFN was determined using a commercial Human Interferon alpha 2 ELISA kit, and the volume of the supernatant was adjusted to achieve a final concentration similar to that of the positive controls (2 nM for the phosphorylation assay and 0.5 nM for the neutralization assay).

Antiviral assay

The antiviral response induced by bacterial supernatants was evaluated as previously described.¹⁷ Briefly, HeLa cells (seeded at 15,000 cells per well) were grown overnight and then subjected to 4-h pre-treatment with serial dilutions of supernatant extracts collected from TOP10 *E. coli* $\Delta dsbA$ expressing either EspC_C or EspC_C+IFN. The cells were then washed and underwent viral challenge using a GFP-expressing lentivirus (VSV-G pseudotyped lentivirus with a pHR-CMV-GFP vector; Table 1) at a multiplicity of infection (MOI) of 1.⁵² Cells were collected 48 h after viral infection and analyzed via FACS to detect GFP-positive cells. The proportion of GFP-expressing cells in the treated samples was quantified relative to that of untreated HeLa cells. Commercial IFN β served as a positive control.

RNA extraction and cDNA preparation

Confluent HeLa cells were incubated for 7 h with filtered supernatants from TOP10 *E. coli* $\Delta dsbA$ bacteria or TOP10 *E. coli* $\Delta dsbA$ expressing EspC_C or EspC_C+IFN. Untreated HeLa cells and HeLa cells incubated with commercial IFN β (2 nM; Pepro-Tech) were used as negative and positive controls, respectively. RNA was extracted from 1×10^6 treated cells using the TRIzol reagent (Invitrogen) and Direct-zol RNA Miniprep kit (Zymo Research) according to the manufacturer's protocol. The extracted RNA was dissolved in RNase-free water, and its integrity was verified through agarose gel electrophoresis. For cDNA synthesis, up to 1 μ g of RNA from each sample was processed using the Protoscript II First Strand cDNA Synthesis Kit (NEB) and the oligo (dT)₂₃ primer, following the protocol provided by the manufacturer.

Quantitative PCR (qPCR)

PCR primer pairs for specific antiviral gene transcripts were designed using the primer BLAST application (NCBI). To reduce the noise caused by DNA contamination, forward and reverse primers were selected from different exons. The primers used for this study are presented in Table 2. RT-qPCR was performed in triplicate using a QuantStudio cycler

(Applied Biotechnologies, Thermo). Each reaction included cDNA produced from cells subjected to the different treatments, gene-specific primers, and SYBR Green I mix (Roche). To evaluate reaction efficiency, a standard curve was constructed for each primer pair by preparing 10-fold serial dilutions of the purified template. The conditions for amplification were: initial denaturation at 95°C for 6 min followed by 35 cycles of 95°C for 15 s, cooling to 58°C for 15 s, and 72°C for 15 s while monitoring fluorescence. Post-amplification melting-curve analyses were performed to confirm reaction specificity. Relative expression levels for each target gene were normalized to the actin housekeeping gene and compared using a double delta Ct analysis. Real-time data were reported as the fold change in relative expression levels.

Statistical analysis

Statistical analysis was performed using IBM SPSS Statistics 29.0. Statistical significance for the antiviral and RT-PCR assays was calculated using an independent 2-tailed t-test with assumed equal variances. Error bars represent the standard deviation.

Results

Identification of the espC domains essential for autotransporter function

To employ EspC as a secretion platform, we initially sought to identify the minimal *espC* sequence necessary for its autotransporter function. The SP and β -barrel domain (Figure 1(b)) have been established as crucial components for secreting the PD.²³ However, whether other EspC domains are essential to this process is unclear. To investigate this unknown, we removed various segments along the PD and examined the secretion of the remaining portions. To detect protein secretion, it was necessary to retain a portion of the PD as a reporter protein, as removing the entire PD would have resulted in the secretion of only a very short peptide due to the cleavage downstream of the SP and upstream of the β -barrel domain, which would have been hard to detect. We, therefore, focused on three similarly-sized segments of the PD: the N-terminal part (NH₂: residues 55–381), middle part (residues 382–708), and C-terminal part (COOH;

residues 709–1004)⁵⁵ (Figure 2). Previous reports suggested that the N-terminal portions of the PD are not required for the secretion of heterologous proteins via the Pet and AIDA proteins.^{25,56} Accordingly, although the serine endopeptidase motif of EspC, located in the PD N-terminal part, is responsible for inducing cellular damage,⁵⁷ this motif has been shown to be non-essential for the release of the PD from the β -barrel domain.³⁴ In contrast, the C-terminal part of the PD, contains an auto-chaperone (AC) domain, which facilitates efficient PD folding and translocation across the outer membrane and is therefore critical for initiating the secretion process.^{28,58–60} Thus, we generated the EspC_{N+C} and EspC_C vectors (Figure 2). The EspC_{N+C} construct included the SP and β -barrel domains, along with the N- and C-terminal portions of the PD. To facilitate the detection of the secreted portion, following the cleavage of the SP and the β -barrel domains, we added a Flag tag downstream from the SP cleavage site. The additional construct, EspC_C, included the SP and β -barrel domains with only the C-part of the PD (Figure 2). As with the EspC_{N+C} construct, a Flag tag was added downstream of the SP sequence to facilitate the detection of C-part secretion. To examine the ability of the EspC_{N+C} and EspC_C constructs to support self-secretion, the plasmids were transformed into three EPEC strains – wildtype (WT) EPEC, the $\Delta espC$, a mutant in which the chromosomal *espC* gene had been deleted, and an EPEC mutant in which the entire locus of enterocyte effacement (LEE), which is crucial for EPEC pathogenicity, was deleted. This latter EPEC Δlee mutant is therefore considered a nonpathogenic strain, making it better suited for protein drug delivery. It has previously been shown that EspC is naturally secreted at high concentrations when the bacteria are grown under T3SS-inducing conditions.^{61–63} Therefore, we grew these strains under similar conditions (tissue culture medium in a CO₂ incubator, statically). To examine the ability of the EspC constructs to express and secrete the PD portions, the bacterial pellets were separated from the culture supernatants by centrifugation, collected, and lysed. The volumes of the supernatants were normalized according to the bacteria's optical density (OD_{600 nm}), filtered, and treated with trichloroacetic acid (TCA) to precipitate the proteins in these samples. We examined the bacterial pellets for protein expression and the supernatants for secretion of the PD portions through SDS-PAGE and western

blotting with an anti-Flag antibody. We observed that both EspC_{N+C} and EspC_C were properly expressed in bacterial pellets, and their processed portions, following the cleavage of the SP and β -barrel domains, were secreted into the extracellular medium (Figure 2). However, EspC_{N+C} secretion differed across strains: it was notably lower in the $\Delta espC$ mutant compared to EPEC WT and Δlee mutant strains, accompanied by a higher full-length protein signal in the bacterial pellet of the $\Delta espC$ mutant (Figure 2). These differences may be attributed to the presence of endogenous EspC protein in WT and Δlee strains, which could facilitate more efficient release of EspC_{N+C} from the membrane-anchored β -barrel. We hypothesize that endogenous EspC can facilitate the proteolytic release of other EspC derivatives *in trans* by cleaving at the conserved motif in the linker region, although this mechanism is not essential for the process. In contrast, EspC_C secretion levels remained consistent across the various EPEC strains. This suggests that the cleavage site within the EspC_C protein may be less accessible compared to EspC_{N+C}. Regardless, these results indicated that the secretion of EspC is not dependent on the N-terminal or middle parts of the EspC PD.

IFN disulfide bonds interfere with EspC-mediated secretion

To examine whether the minimized EspC_C design can support the secretion of a recombinant protein, we inserted the coding sequence for human IFN α 2 into the EspC_C construct. We used the IFN α 2 YNS version, which reportedly exhibits enhanced activity.⁴³ We found that the EspC_C+IFN fusion protein was expressed in all EPEC strains (WT, $\Delta espC$, and Δlee). However, while the EspC_C construct facilitated the secretion of the C-terminal portion into the culture medium, the fused construct consisting of the C-terminus and IFN was not secreted (Figure 3). A likely explanation for this lack of IFN secretion could be the presence of disulfide bonds in the IFN protein. Studies have shown that T5SS proteins typically contain a limited number of cysteine residues within their PDs, and when present, these residues are often located close to one another.^{23,33,64} It has previously been suggested that recombinant proteins with disulfide bonds, such as IFN α 2, might pose a barrier to the autotransporters' secretion mechanism. Disulfide bond formation induces the partial

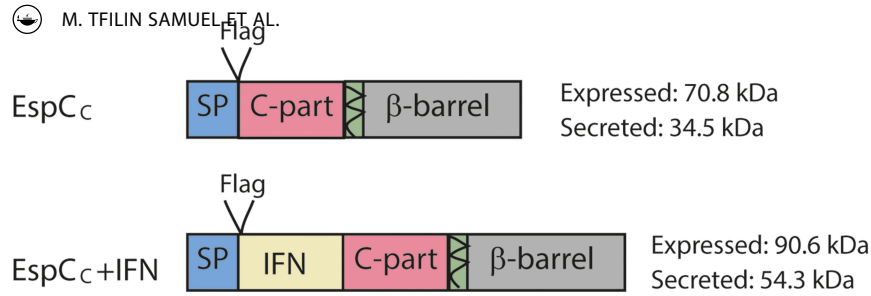
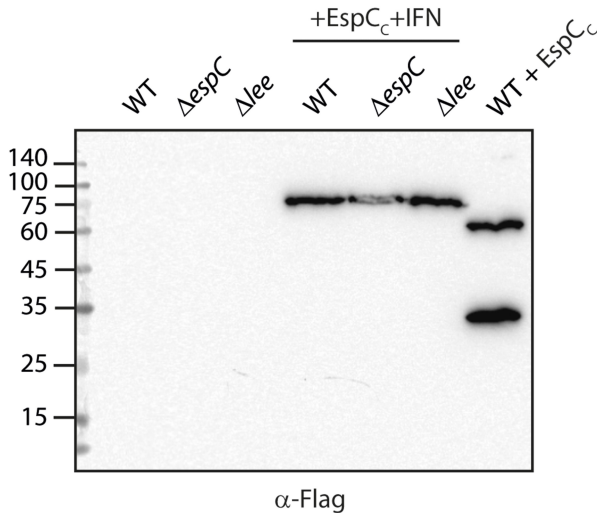
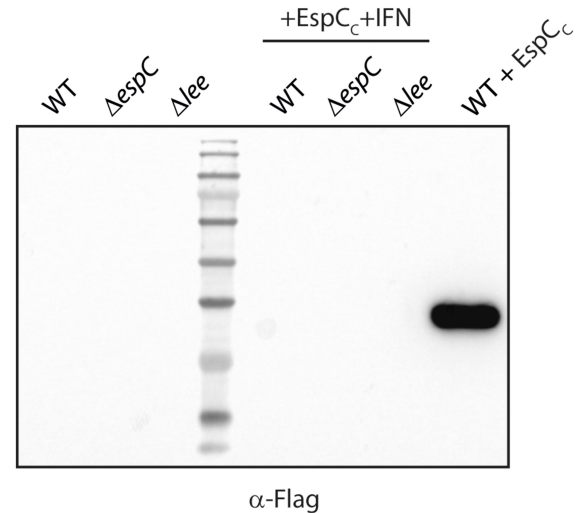
**Bacterial pellets:****Supernatants:**

Figure 3. The EspC_C+IFN construct is not secreted into EPEC culture supernatants. Domain organization of the EspC_C+IFN protein and its expected sizes, as a precursor and a secreted protein, are presented along the EspC_C protein. The EspC_C+IFN construct was transformed into EPEC wildtype (WT), *ΔespC*, and *Δlee* strains, which were grown for 6 h. The cultures were centrifuged, and the supernatants and pellets were separated. The secreted fractions were normalized according to OD₆₀₀ values, concentrated, and analyzed along with the bacterial pellets by SDS-PAGE and western blotting with an anti-flag antibody. The expression (left panel, bacterial pellets) and EspC-mediated secretion (right panel, supernatants) demonstrated secretion of the cargo-free EspC_C construct but not of the one fused to IFN.

folding of the precursor protein, which hinders its translocation across the outer membrane.³² Although SPATE autotransporters, such as Pet, EspP, and EspC, contain cysteine residues capable of forming disulfide bonds, the cysteine pairs involved in these bonds are separated by no more than 20 residues.⁶⁵ Therefore, we hypothesized that the two disulfide bonds in IFNα2 - formed between cysteines at positions 1 and 99, and positions 29 and 139, which are separated by more than 90 residues⁶⁶ - might interfere with the ability of this construct to be secreted via the EspC autotransporter due to the protein partial folding.

IFN can be secreted via EspC when expressed in a *ΔdsbA* mutant strain

To test our hypothesis that disulfide bond formation interferes with IFN secretion via the EspC autotransporter, we utilized a bacterial strain (TOP10 *E. coli*) that is deficient in its ability to create disulfide bonds due to the deletion of the *dsbA* gene. This gene encodes the periplasmic protein that mediates disulfide bond formation in *E. coli*.⁶⁷ Since EspC secretion operates independently of EPEC-specific components, we anticipated that the system would function in alternative *E. coli* strains, such as the TOP10

E. coli strain. Additionally, the TOP10 strain is considered safer than the nonpathogenic Δ lee EPEC mutant, making it better option for further development. In addition, we constructed a new vector, EspC+IFN, in which the IFN coding sequence was directly inserted between the SP and β -barrel domains, without the C-terminal part of the PD (Figure 4(a)). This construct allowed us to investigate whether the C-part of the PD is crucial for EspC-mediated secretion. The EspC+IFN and EspC_C+IFN plasmids were transformed into TOP10 *E. coli* WT and Δ dsbA mutant strains to determine their ability to support IFN secretion. We found that expression of the EspC_C+IFN construct in the TOP10 *E. coli* Δ dsbA mutant facilitated significant secretion of IFN to the culture medium (~60 ng/mL in cultures grown under conditions described in the materials and methods, quantified by ELISA) while only minimal secretion was observed when the EspC_C+IFN construct was expressed in WT TOP10 *E. coli*. The high DnaK signal observed in the supernatant sample of the WT strain suggested that the minimal IFN signal resulted from limited bacterial lysis and not from the active secretion of IFN. Furthermore, we found that the expression of the EspC+IFN construct in the Δ dsbA mutant strain did not facilitate IFN secretion (Figure 4(c)). This suggests that the EspC+IFN construct, which lacks the C-terminal portion of the PD, is insufficient for secretion via the EspC autotransporter. It is, therefore, likely that the C-terminal portion of the PD contains crucial components that are required for EspC-mediated secretion. These results are consistent with the role of the AC domain, found in the C-terminal part of the PD, in facilitating passenger domain folding and translocation.^{28,58} Additionally, we can conclude that TOP10 *E. coli* Δ dsbA allows effective protein secretion via the EspC protein when the transported cargo contains disulfide bonds.

Secreted EspC_C+IFN induces JAK-STAT signal transduction in vitro

After detecting IFN fused to the C-terminal portion of PD in the supernatant fraction of TOP10 *E. coli* Δ dsbA, we examined whether this secreted IFN was functional. The binding of IFN to its receptor, IFNAR, activates the JAK-STAT signaling

pathway, resulting in phosphorylation of the cellular STAT2 protein.⁶⁸ To examine the functionality of EspC-secreted IFN, we incubated Caco-2 and HT-29 cells with filtered supernatants from TOP10 *E. coli* Δ dsbA strain expressing EspC_C, EspC_C+IFN, or EspC+IFN. The IFN concentration in the supernatant of EspC_C+IFN was quantified by ELISA and added to cells at 2 nM final concentration. Equivalent volumes of EspC_C and EspC+IFN supernatants were used for comparison. Recombinant IFN β was used as a positive control, as the bacterial-secreted IFN α used in this study is considered an 'IFN β -like' version. The cells were then collected and subjected to SDS-PAGE and western blotting analyses with α -phosphorylated-STAT2 antibody (p-STAT2) to detect the ability of IFN to initiate the JAK-STAT response. We found that cells incubated with supernatants from bacteria that secrete the EspC_C+IFN protein triggered STAT2 phosphorylation, much like cells incubated with commercial IFN β (Figure 5(a,b)). In contrast, no phosphorylation (in HT-29) or very low levels of phosphorylation (in Caco-2) were observed with supernatants of bacteria that expressed either EspC_C or EspC+IFN (Figure 5(a,b)). The low STAT phosphorylation signal observed in Caco-2 cells incubated with EspC+IFN supernatant may result from limited bacterial lysis and subsequent low IFN concentration (Figure 4(c)), due to the overexpression of the EspC derivative. To validate that STAT2 phosphorylation was specifically induced by bacterially secreted IFN, we examined the ability of an anti-IFN α 2 antibody to neutralize the effect of the IFN found in the supernatants of TOP10 *E. coli* Δ dsbA expressing EspC_C+IFN. Using the human Interferon alpha 2 ELISA kit, we first measured the concentration of IFN in the bacterial supernatant. Caco-2 cells were treated with bacterial supernatants containing IFN or commercial IFN α 2 (0.5 nM). These samples were pre-incubated with a 10-fold excess (5 nM) of anti-IFN α 2 before application to the cells to assess antibody neutralization. As expected, we observed that the addition of recombinant IFN α 2 (0.5 nM) induced robust STAT2 phosphorylation, while very low levels of p-STAT2 were observed in untreated cells or cells incubated with the supernatants of bacteria expressing EspC_C (Figure 5(c)). Furthermore, we found that pre-incubation of

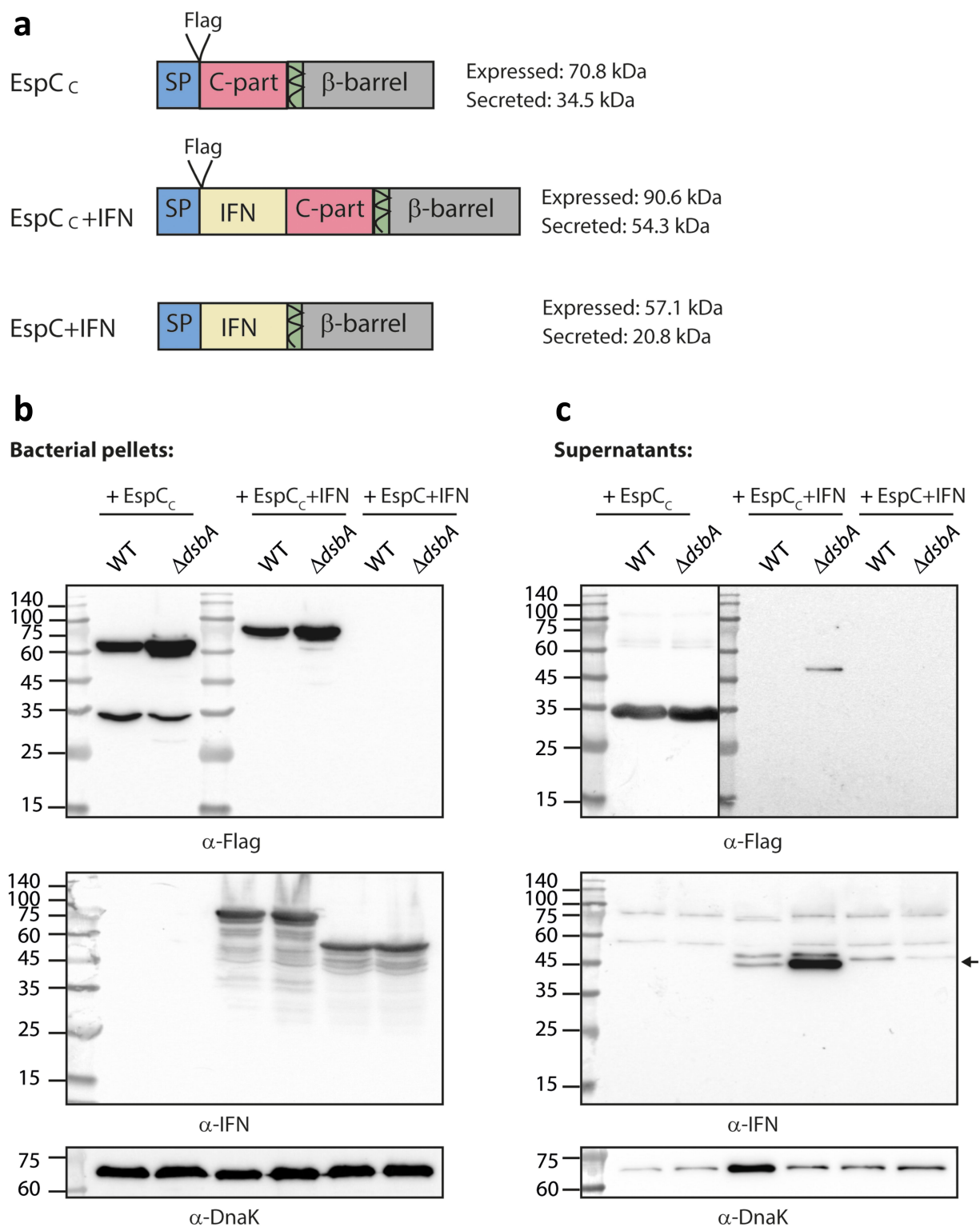


Figure 4. The EspC_C+IFN construct supports IFN secretion when expressed in $\Delta dsbA$ mutant *E. coli*. (a) Domain organization of the EspC_C+IFN and EspC+IFN proteins and their expected sizes, as precursors and secreted proteins, are presented along the EspC_C protein. (b–c) the constructs were transformed into TOP10 *E. coli* wildtype (WT) and $\Delta dsbA$ mutant (deficient in disulfide bond formation) strains, which were grown for 6 h. The cultures were centrifuged to separate the supernatants and the pellets. Bacterial pellets (b) and normalized supernatants (c) were analyzed by SDS-PAGE and western blotting with anti-flag, anti-IFN α 2, and anti-DnaK antibodies. The results demonstrated that IFN can be secreted into the culture supernatant when expressed using the EspC_C+IFN construct in the TOP10 *E. coli* $\Delta dsbA$ mutant. An arrow indicates the position of secreted EspC_C+IFN.

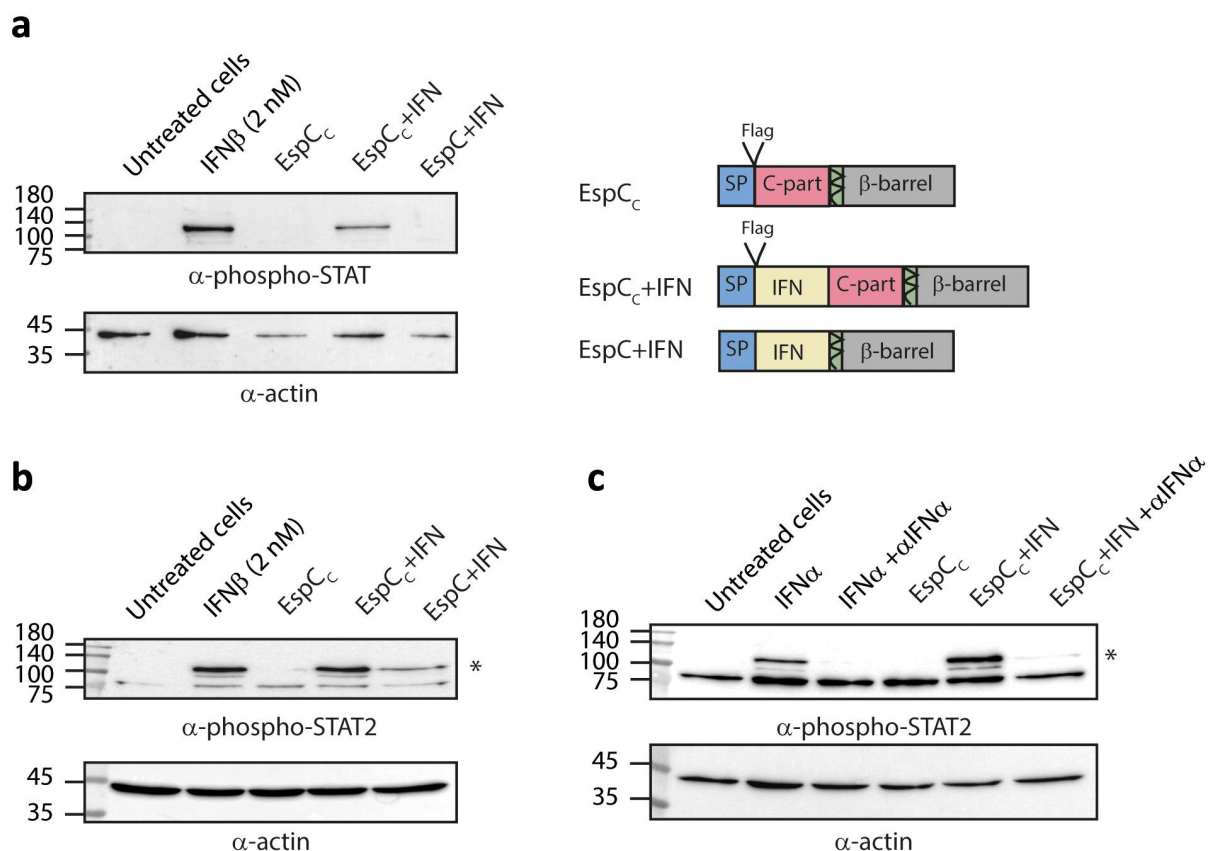


Figure 5. EspC-secreted IFN induces IFNAR activation pathway. HT-29 (a) and Caco-2 (b) cells were incubated with supernatants of *E. coli* TOP10 Δ *dsbA* transformed with Esp C_C , Esp C_C +IFN, or EspC+IFN (protein schemes are presented in panel a). The cells were washed, lysed, and their protein extracts were subjected to SDS-PAGE and western blot analysis using anti-phosphorylated STAT2 (phospho-stat) and anti-actin (loading control) antibodies. Cells incubated with commercial IFN β (2 nM) were used as a positive control, while a sample of untreated cells was used as a negative control. A strong pSTAT signal was observed in cells that were incubated with *E. coli* TOP10 Δ *dsbA* supernatants expressing the Esp C_C +IFN protein. (c) Caco-2 cells were incubated with supernatants of *E. coli* TOP10 Δ *dsbA* expressing the Esp C_C +IFN protein (0.5 nM) or with commercial IFN α 2 (0.5 nM), alone or following pre-incubation with an anti-IFN α 2 antibody (5 nM) for 1 h. IFN α 2 (0.5 nM) was used as a positive control, and untreated cells and cells incubated with supernatant of *E. coli* TOP10 Δ *dsbA* expressing Esp C_C were used as a negative control. pSTAT signal was observed in cells incubated with supernatants of *E. coli* TOP10 Δ *dsbA* expressing the Esp C_C +IFN protein, while neutralizing antibody eliminated STAT2 phosphorylation.

commercial IFN α 2 or Esp C_C +IFN-containing supernatants with the neutralizing antibody almost completely eliminated STAT2 phosphorylation (Figure 5(c)). These findings suggest that IFN can be secreted via the EspC platform, and although it is fused to the C-terminal portion of the PD, it is biologically active.

EspC-secreted IFN induces ISG transcription

To evaluate the effect of Esp C_C +IFN on gene regulation, we examined changes in the levels of transcriptional activity for three antiviral ISGs – OAS2, MX2, and PKR. Since gut epithelial cells, such as Caco-2 and HT-29, may be less sensitive to IFN

stimulation,⁶⁹ we incubated bacterial supernatants with HeLa cells. Samples of untreated HeLa cells or HeLa cells treated with commercial IFN β (2 nM) served as negative and positive controls, respectively. Our results showed that the exposure of HeLa cells to a supernatant containing the Esp C_C +IFN protein induced a significant upregulation of antiviral ISGs at the mRNA level. However, the upregulation of OAS2 and MX2 was not as significant as that induced by commercial IFN β (Figure 6). This difference can be attributed to the Esp C_C +IFN design, which resulted in secreted IFN fused to the PD's C-terminal portion. This fusion may interfere with the efficient binding of IFN to IFNAR, thus leading to a reduced response.

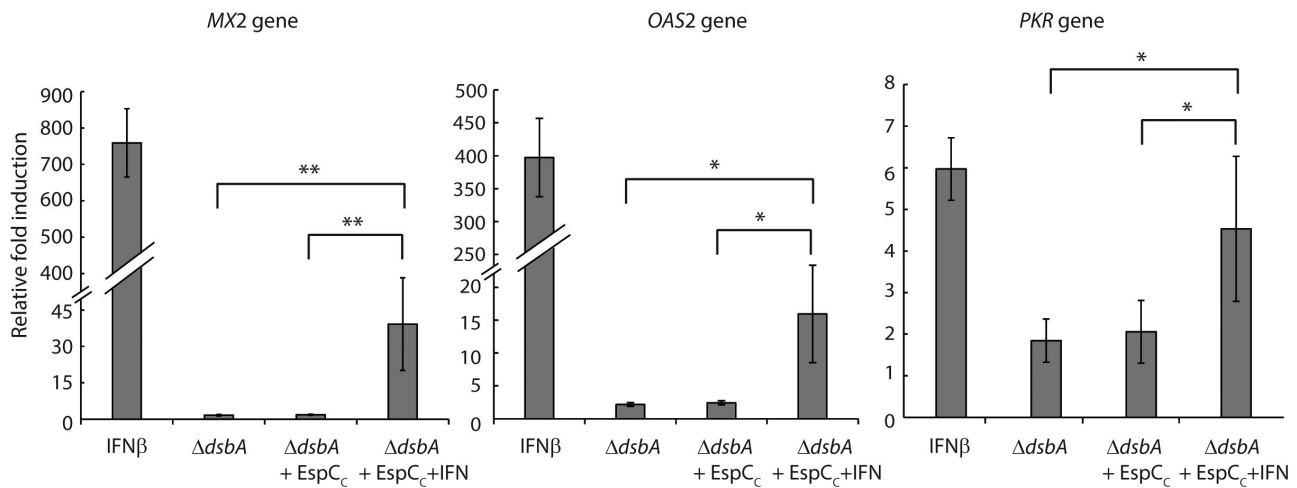


Figure 6. EspC-secreted IFN induces the transcription of interferon-stimulated antiviral genes. HeLa cells were incubated with bacterial supernatants of *E. coli* TOP10 $\Delta dsbA$ or $\Delta dsbA$ expressing either EspC_C ($\Delta dsbA + EspC_C$) or EspC_C+IFN ($\Delta dsbA + EspC_C + IFN$). Cells incubated with commercial IFN β (2 nM) served as a comparative reference. Transcription levels of three interferon-stimulated genes (MX2, OAS2, and PKR) were determined by RT-PCR and are presented as fold induction relative to untreated cells. Results represent at least 4 independent biological replicates. Bars represent the standard error, * $p < 0.05$, ** $p < 0.01$.

Another potential explanation for the reduced ISG upregulation by EspC_C+IFN is the absence of disulfide bonds in the secreted IFN protein due to its expression in the $\Delta dsbA$ background. However, our recent findings demonstrated that IFN secreted by the T3SS – which bypasses the periplasm and thus does not form disulfide bonds, remaining in an unfolded conformation – induces ISG upregulation similar to commercial IFN β .¹⁷ These results suggest that the secreted IFN can form spontaneous disulfide bonds extracellularly, independent of the DsbA enzyme. We expect a similar process to occur with EspC_C+IFN, unless the fusion of IFN to the C-part of the PD interferes with it. Incubation of HeLa cells with TOP10 *E. coli* $\Delta dsbA$ and TOP10 *E. coli* $\Delta dsbA$ expressing the EspC_C protein also induced enhanced ISG transcription, albeit at levels significantly lower than those induced by commercial IFN β or the supernatants containing EspC_C+IFN (Figure 6). This more limited upregulation likely represents the cellular response to general bacterial components, such as LPS, which can trigger the autocrine and paracrine secretion of type I IFNs by cells.⁷⁰ There was no substantial difference in gene regulation between samples of cells incubated with supernatants of TOP10 *E. coli* $\Delta dsbA$ versus supernatants of TOP10 *E. coli* $\Delta dsbA$ expressing EspC_C (Figure 6). These results suggest that the C-terminal portion of PD by itself does not trigger an antiviral response in cells. They

also confirm that the observed upregulation of ISGs in HeLa cells incubated with EspC_C+IFN supernatants was specifically induced by EspC-secreted IFN, rather than a response to general bacterial components present in the supernatants.

EspC_C+IFN induces an antiviral effect in HeLa cells

The activation of the IFN signaling pathway is essential to mount a robust defense response against viral infections. Upon activation, it upregulates the expression of antiviral ISGs, which enhance cellular resistance to viral invasions. To assess the antiviral response *in vitro*, we used a GFP-expressing pseudovirus model to infect HeLa cells. This modified VSV-G pseudotyped virus was designed to efficiently transduce target cells but lacks the ability to complete the viral replication cycle or generate new progeny virions. Using this model, we tested whether bacterially secreted IFN could enhance the antiviral response. To do this, cells were pre-incubated for 4 h with concentrated or diluted supernatants from TOP10 *E. coli* $\Delta dsbA$ expressing either EspC_C+IFN or EspC_C. The cells were then washed and infected with the GFP-expressing pseudovirus (MOI = 1) for 48 h. Thereafter, the cells were harvested and subjected to FACS analysis to determine the percentage of GFP-positive cells, which indicates viral infection. The percentage of GFP-positive cells

treated with bacterial supernatants was normalized relative to the level of GFP-positive untreated HeLa cells. We found that cells treated with supernatants of bacteria expressing EspC_C+IFN showed reduced viral entry compared to untreated cells (60%), while the cells incubated with the supernatants of bacteria expressing EspC_C exhibited a similar number of GFP-positive cells as the untreated cells upon viral infection (Figure 7(a)). These results indicate that EspC_C+IFN can stimulate an antiviral response in HeLa cells and subsequently reduce viral entry into cells in a dose-dependent manner. To present the antiviral activity as a function of IFN concentration, we plotted the results based on the IFN concentration in the EspC_C+IFN supernatants and compared them to the percentage of GFP-positive cells after treatment with recombinant IFN β (Figure 7(b)). The results suggested that the bacterially secreted EspC_C+IFN triggers an antiviral response similar to that elicited by IFN β . Representative immunofluorescence images showed that cells infected with viral particles without pre-treatment display a higher percentage of GFP-positive cells. In contrast, cells pre-incubated with the bacterial extract from TOP10 *E. coli* $\Delta dsbA$ expressing EspC_C+IFN exhibit a reduced percentage of GFP-positive cells comparable to that for cells pretreated with IFN β (Figure S1). Cells pre-incubated with the bacterial extract from TOP10 *E. coli* $\Delta dsbA$ expressing EspC_C showed a minimal reduction in GFP-positive cells compared to untreated cells (Figure S1). These results indicate that nonpathogenic bacteria can secrete EspC_C+IFN, bind to cellular IFNAR, and activate signal transduction, resulting in STAT2 phosphorylation and ISG upregulation, which initiates an antiviral response.

EspC_C+IFN can be secreted under culture conditions simulating gut

To assess whether EspC-mediated secretion can occur in the GIT, we tested the secretion of EspC_C+IFN under gut-simulating conditions *in vitro*. To that end, TOP10 *E. coli* $\Delta dsbA$ carrying either the EspC_C or the EspC_C+IFN plasmids were grown anaerobically in DMEM supplemented with

various dilutions of synthetic fecal stool media (1:1, 1:5, and 1:10). In addition, the strains were grown anaerobically in full DMEM as a control, as this medium has been previously shown to induce EspC-mediated secretion under aerobic conditions. We observed that EspC_C+IFN was secreted to varying degrees in all tested conditions

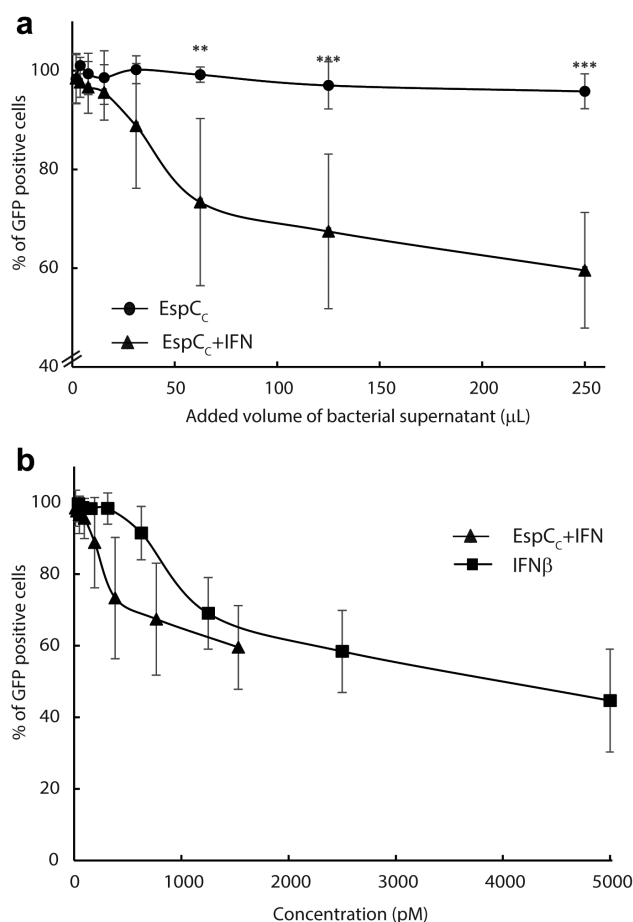


Figure 7. Bacterially secreted EspC_C+IFN exhibits antiviral activity. HeLa cells were incubated with extracts of bacterial supernatants from TOP10 *E. coli* $\Delta dsbA$ expressing either EspC_C or EspC_C+IFN for 4 h before being washed and transduced with a GFP-expressing pseudovirus at an MOI of 1. Cells were harvested 48 h post-transduction and subjected to FACS analysis to assess GFP expression. The results are presented as the percentage of GFP-positive cells relative to GFP-positive cells in the untreated control sample, which was not pre-incubated with bacterial supernatants. The antiviral activity is presented as a function of the volume of the bacterial extracts (a) or IFN concentration (b). The antiviral activity of recombinant IFN β is also depicted in (b), serving as a comparative reference for the activity of bacterially-secreted IFN and showing that secreted EspC_C+IFN triggers an antiviral response similar to that elicited by IFN β . Bars represent the standard deviation, * $p < .01$, ** $p < .001$.

(Figure 8(a)). The strongest secretion occurred in bacteria grown in full DMEM, with a gradual reduction as the proportion of synthetic fecal

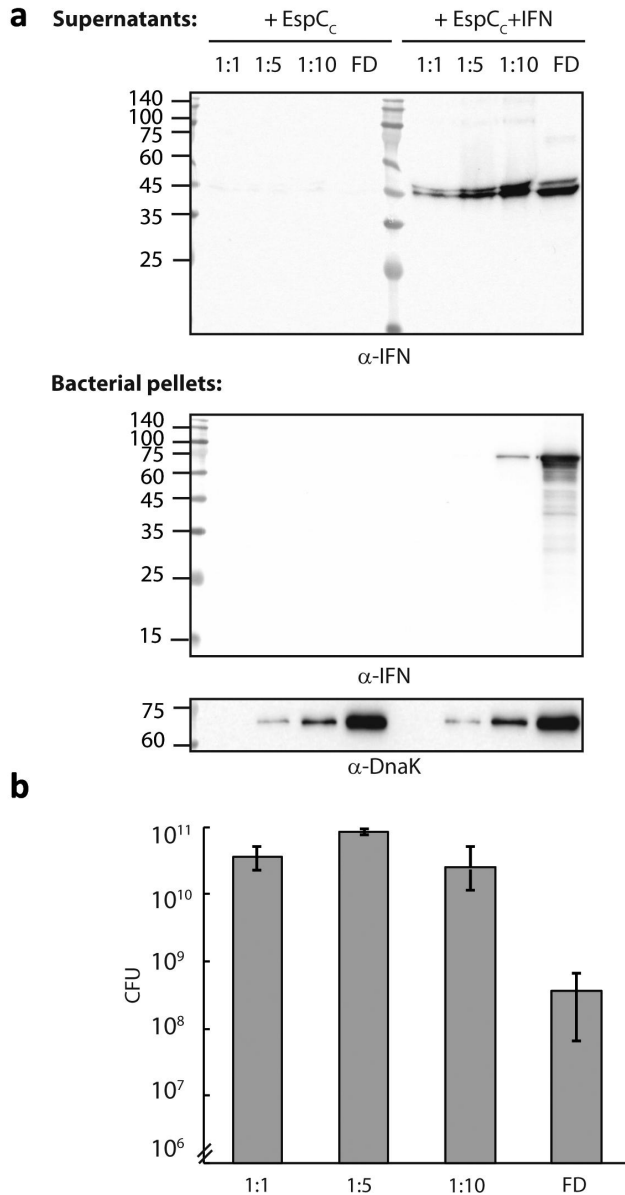


Figure 8. Esp_{C_c}+IFN is secreted under culture conditions simulating gut. TOP10 *E. coli* Δ dsbA expressing either Esp_{C_c} or Esp_{C_c}+IFN proteins were grown anaerobically in full DMEM (FD) and in various dilutions of synthetic fecal stool media (1:1, 1:5, and 1:10) for 6 h. Protein expression was induced by IPTG (0.1 mM). (a) The cultures were centrifuged to separate the supernatants and the pellets. Bacterial pellets (upper panel) and normalized supernatants (lower panel) were analyzed by SDS-PAGE and western blotting with anti-IFN and anti-DnaK antibodies, demonstrating that IFN can be secreted into the culture supernatant under gut-simulating conditions. (b) Samples were collected from bacterial cultures after 6 h growth under anaerobic conditions and plated on LB agar supplemented with carbenicillin. CFUs were counted and are presented in the graph (logarithmic scale). Bars represent the standard deviation.

material in the medium increased. Surprisingly, while IFN was consistently detected in the supernatants of bacteria carrying the Esp_{C_c}+IFN plasmid under all growth conditions, high Esp_{C_c}+IFN expression was only observed in the bacterial pellet when grown in full DMEM. Bacteria grown in the 1:10 dilution of synthetic fecal medium exhibited partial expression, whereas no expression was detected in the 1:1 and 1:5 dilutions (Figure 8(a)). To confirm that the addition of synthetic fecal material to the culture medium does not affect bacterial fitness, we collected samples at the end of the growth period, plated them on agar plates, and quantified colony-forming units (CFUs). We observed that supplementation of DMEM with synthetic fecal material enhanced TOP10 *E. coli* Δ dsbA growth by at least one-fold (Figure 8(b)). These results excluded the possibility that the lack of Esp_{C_c}+IFN signal in the western blots of the bacterial pellets was due to a defect in protein production or growth inhibition. To investigate this discrepancy between protein secretion and expression, given that protein expression is a prerequisite for secretion, we also analyzed the bacterial pellets for DnaK, a housekeeping protein used as a marker for bacterial growth. Western blotting revealed a pattern similar to that of IFN expression in the bacterial pellets, showing that samples grown in media with higher levels of synthetic fecal content had reduced levels of DnaK (Figure 8(a)). The lack of correlation between CFU counts of cultures supplemented with synthetic feces (Figure 8(b)) and the DnaK level in western blots of the bacterial pellets suggests that the reduced Esp_{C_c}+IFN signal in the pellets was due to less effective detection and technical limitations rather than decreased protein expression. These limitations may stem from the presence of residual salts or metabolites originating from the synthetic fecal medium, which interfere with antibody binding, as previously reported.⁷¹ Interestingly, this issue was not observed in the supernatant samples, likely because these samples were pretreated with TCA, which helps precipitate proteins and dissociate them from salts and metabolites.⁷² This suggests that while synthetic feces can complicate protein detection in bacterial lysates, it does not interfere with the ability to detect secreted proteins in the culture supernatants. Our

results indicate that EspC_C+IFN can be secreted under gut-simulating conditions *in vitro*. This supports the feasibility of using an EspC-mediated system to deliver biologics *in vivo*.

Discussion

In recent years, several strategies have been developed for the oral administration of biologics to overcome challenges related to the breakdown and inactivation of these drugs as they pass through the GIT.¹ Several techniques have been developed for the oral delivery of biologics, however, those methods are costly and may reduce drug efficacy.^{1,3} To address these challenges, researchers, including our team, have explored using bacteria as a delivery platform for these drugs. This approach leverages the ability of some bacteria to survive the harsh conditions of the stomach and produce the drug directly in the GIT, using genetically engineered bacteria that express and secrete therapeutic proteins or peptides.^{4,5} Bacterial secretion systems, such as the T3SS, are a promising option for engineering bacteria to secrete biologics.^{9–11} However, some of these secretion systems are used as virulence mechanisms, expressed by pathogenic bacteria, or contain complex machinery.^{9–11}

This study presents the relatively simple secretion system, T5SS, as a novel method for secreting functional IFN using the EspC autotransporter. The EspC is a unique secretion apparatus because it relies on the expression of a single protein. We discovered that the full EspC sequence is not essential for recombinant protein secretion; notably, both the N-terminal and middle regions are dispensable for this process (Figure 2). These findings indicate that large segments of EspC's passenger domain can be removed while preserving its capacity to secrete the cargo protein, unlike another *E. coli* autotransporter, Hemoglobin protease.⁴⁴ However, fusing IFN to the C-terminal part of the EspC PD disrupted the ability of the PD to be secreted. To determine whether this inability resulted from disulfide bonds formed within the IFN protein,^{23,33} we examined the ability of EspC_C+IFN to be secreted when expressed in the TOP10 *E. coli* $\Delta dsbA$ mutant, which is deficient in disulfide bond formation. The $\Delta dsbA$ mutant facilitated efficient IFN secretion via EspC (Figure 4), thus confirming that this strain can be used as a delivery

platform for disulfide-bond-containing proteins using the EspC platform.

To establish that the bacterial-secreted IFN was functional, we examined its ability to activate the JAK-STAT signaling pathway and upregulate ISGs. We found that the supernatants of TOP10 *E. coli* $\Delta dsbA$ expressing EspC_C+IFN induced the phosphorylation of STAT2 and the upregulation of antiviral genes (Figures 5 and 6). Interestingly, HeLa cells treated with commercial IFN β exhibited significantly higher levels of OAS2 and MX2 transcription as compared to those treated with EspC_C+IFN supernatants, although the IFN YNS version used in this study was previously reported to induce a stronger antiviral response in WISH cells than that elicited by IFN β .⁴³ We speculate that this reduced ISG upregulation induced by EspC_C+IFN compared to the IFN β is due to the presence of the ~30 kDa PD C-part fused to the C-terminal region of IFN. This fusion may alter the affinity with which IFN binds to IFNAR, as previous studies have demonstrated that weaker binding of IFN α subtypes to the receptor results in the less pronounced upregulation of antiviral genes.^{73,74} Furthermore, the binding of IFN α 2 to IFNAR has been shown to involve residues at the C-terminus of IFN α 2.⁷⁵ Therefore, it is probable that the fusion of the C-part of the PD at this critical region of IFN reduces its affinity for its cognate receptor. To address this issue, we plan to add an additional protease cleavage site between IFN and the C-part of PD, which will release the mature form of IFN from the interfering C-part upon secretion.³⁷ This cleavage site could either be a second proteolytic motif similar to the one present in the linker domain of EspC or a more general cleavage site, such as one recognized by trypsin. We speculate that this addition will enhance the biological activity of the secreted IFN. Despite the relatively mild upregulation of antiviral genes by the EspC-secreted IFN, it stimulated a sufficient antiviral response that significantly reduced the viral infection of cells (Figure 7). These results suggest that although EspC_C+IFN may have a lower affinity for IFNAR, it can still induce a transcriptional response strong enough to activate a full antiviral cellular response.⁷⁴ This aligns with a previous study showing that partial STAT activation is sufficient to confer complete antiviral protection,⁷⁴

implying that antiviral gene transcription levels are not linearly linked to cellular resistance to viral infections.

Overall, this study introduces an innovative delivery method for IFN that holds the potential for further development for oral administration of the drug, offering a promising alternative to the current IFN parenteral treatment strategies and improving patient compliance.^{42,43} We have demonstrated that IFN secretion can be facilitated by nonpathogenic bacteria using the EspC protein, overcoming IFN structural limitations, and that bacterial-secreted IFN can activate IFN signal transduction *in vitro*. We plan to move to an animal model to examine the ability of bacterially secreted IFN to cross the mucus layer and reach the epithelium and possibly the bloodstream. For these analyses, we will construct a plasmid that encodes murine IFN α , which shares ~50% similarity with human IFN and its corresponding receptors.⁷⁶ These secreting bacteria will be used to assess IFN levels in the intestinal lumen and bloodstream *in vivo*, when given orally to mice, as well as to evaluate its potential toxicity on the host. Since TOP10 *E. coli* do not colonize the intestine, administration of these bacteria would provide a transient effect. We hypothesize that optimizing the bacterial titers administered and/or fine-tuning the regulatory elements controlling IFN expression could reduce toxicity while maintaining its therapeutic efficacy. Additionally, the transient retention of the bacteria within the host would allow for more precise regulation of IFN levels, minimizing the risk of toxicity or overactivation of the immune system and enabling more controlled, dose-dependent therapeutic outcomes. The murine model will ideally validate the potential of using the EspC-based method as a promising platform for the delivery of various biologics, potentially encouraging its broader application in biotechnology and medicine.

Disclosure statement

No potential conflict of interest was reported by the author(s).

Funding

The work was supported by the Israel Science Foundation [988/19]; Ministry of Science and Technology, Israel [3-16841].

ORCID

Ran Taube  <http://orcid.org/0000-0002-2062-4537>

Neta Sal-Man  <http://orcid.org/0000-0002-1109-479X>

Data availability statement

The authors confirm that the data supporting the findings of this study are available within the article and are openly available on figshare.com at https://figshare.com/articles/figure/_/27878025.

References

1. Mehrotra S, Kalyan Bg P, Nayak PG, Joseph A, Manikkath J. Recent progress in the oral delivery of therapeutic peptides and proteins: overview of pharmaceutical strategies to overcome absorption hurdles. *Adv Pharm Bull.* 2024;14:11–33. doi:10.34172/apb.2024.009.
2. Wright L, Barnes TJ, Prestidge CA. Oral delivery of protein-based therapeutics: gastroprotective strategies, physiological barriers and *in vitro* permeability prediction. *Int J Pharm.* 2020;585:119488. doi:10.1016/j.ijpharm.2020.119488.
3. Cao SJ, Xu S, Wang HM, Ling Y, Dong J, Xia RD, Sun XH. Nanoparticles: oral delivery for protein and peptide drugs. *AAPS PharmSciTech.* 2019;20(5):190. doi:10.1208/s12249-019-1325-z.
4. Hosseiniidoust Z, Mostaghaci B, Yasa O, Park BW, Singh AV, Sitti M. Bioengineered and biohybrid bacteria-based systems for drug delivery. *Adv Drug Deliv Rev.* 2016;106:27–44. doi:10.1016/j.addr.2016.09.007.
5. Riglar DT, Silver PA. Engineering bacteria for diagnostic and therapeutic applications. *Nat Rev Microbiol.* 2018;16(4):214–225. doi:10.1038/nrmicro.2017.172.
6. Claesen J, Fischbach MA. Synthetic microbes as drug delivery systems. *ACS Synth Biol.* 2015;4(4):358–364. doi:10.1021/sb500258b.
7. Burdette LA, Leach SA, Wong HT, Tullman-Ercek D. Developing gram-negative bacteria for the secretion of heterologous proteins. *Microb Cell Fact.* 2018;17(1):196. doi:10.1186/s12934-018-1041-5.
8. Green ER, Meccas J. Bacterial secretion systems: an overview. *Microbiol Spectr.* 2016;4(1). doi:10.1128/microbiolspec.VMBF-0012-2015.
9. Chamekh M, Phalipon A, Quertainmont R, Salmon I, Sansonetti P, Allaoui A. Delivery of biologically active anti-inflammatory cytokines IL-10 and IL-1ra *in vivo* by the Shigella type III secretion apparatus. *J Immunol.* 2008;180(6):4292–4298. doi:10.4049/jimmunol.180.6.4292.
10. Shi L, Yu B, Cai CH, Huang JD. Angiogenic inhibitors delivered by the type III secretion system of tumor-targeting *Salmonella typhimurium* safely shrink

- tumors in mice. *AMB Express*. 2016;6(1):56. doi:10.1186/s13568-016-0226-8.
11. Walker BJ, Stan GV, Polizzi KM. Intracellular delivery of biologic therapeutics by bacterial secretion systems. *Expert Rev Mol Med*. 2017;19:e6. doi:10.1017/erm.2017.7.
 12. Deng W, Marshall NC, Rowland JL, McCoy JM, Worrall LJ, Santos AS, Strynadka NCJ, Finlay BB. Assembly, structure, function and regulation of type III secretion systems. *Nat Rev Microbiol*. 2017;15(6):323–337. doi:10.1038/nrmicro.2017.20.
 13. Ham H, Orth K. The role of type III secretion system 2 in *Vibrio parahaemolyticus* pathogenicity. *J Microbiol*. 2012;50(5):719–725. doi:10.1007/s12275-012-2550-2.
 14. Marteyn B, Gazi A, Sansonetti P. Shigella: a model of virulence regulation in vivo. *Gut Microbes*. 2012;3(2):104–120. doi:10.4161/gmic.19325.
 15. Sal-Man N, Setiawati D, Scholz R, Deng W, Yu AC, Strynadka NC, Finlay BB. EscE and EscG are cochaperones for the type III needle protein EscF of enteropathogenic *Escherichia coli*. *J Bacteriol*. 2013;195(11):2481–2489. doi:10.1128/JB.00118-13.
 16. Bai F, Li Z, Umezawa A, Terada N, Jin S. Bacterial type III secretion system as a protein delivery tool for a broad range of biomedical applications. *Biotechnol Adv*. 2018;36(2):482–493. doi:10.1016/j.biotechadv.2018.01.016.
 17. Rostovsky I, Wieler U, Kuzmina A, Taube R, Sal-Man N. Secretion of functional interferon by the type 3 secretion system of enteropathogenic *Escherichia coli*. *Microb Cell Fact*. 2024;23(1):163. doi:10.1186/s12934-024-02397-y.
 18. Gonzalez-Prieto C, Lesser CF. Rationale redesign of type III secretion systems: toward the development of non-pathogenic *E. coli* for in vivo delivery of therapeutic payloads. *Curr Opin Microbiol*. 2018;41:1–7. doi:10.1016/j.mib.2017.10.011.
 19. Beriotto I, Icke C, Sevastyanovich YR, Rossiter AE, Romagnoli G, Savino S, Hodges FJ, Cole JA, Saul A, MacLennan CA, et al. Efficient autotransporter-mediated extracellular secretion of a heterologous recombinant protein by *Escherichia coli*. *Microbiol Spectr*. 2023;11(3):e0359422. doi:10.1128/spectrum.03594-22.
 20. Byrd W, Ruiz-Perez F, Setty P, Zhu C, Boedeker EC. Secretion of the Shiga toxin B subunit (Stx1B) via an autotransporter protein optimizes the protective immune response to the antigen expressed in an attenuated *E. coli* (rEPEC E22Δler) vaccine strain. *Vet Microbiol*. 2017;211:180–188. doi:10.1016/j.vetmic.2017.10.006.
 21. Clarke KR, Hor L, Pilapitiya A, Luirink J, Paxman JJ, Heras B. Phylogenetic classification and functional review of autotransporters. *Front Immunol*. 2022;13:921272. doi:10.3389/fimmu.2022.921272.
 22. Fan E, Chauhan N, Udatha D, Leo JC, Linke D. Type V secretion systems in bacteria. *Microbiol Spectr*. 2016;4(1). doi:10.1128/microbiolspec.VMBF-0009-2015.
 23. Henderson IR, Navarro-Garcia F, Nataro JP. The great escape: structure and function of the autotransporter proteins. *Trends Microbiol*. 1998;6(9):370–378. doi:10.1016/S0966-842X(98)01318-3.
 24. Meuskens I, Saragliadis A, Leo JC, Linke D. Type V secretion systems: an overview of passenger domain functions. *Front Microbiol*. 2019;10:1163. doi:10.3389/fmicb.2019.01163.
 25. Sevastyanovich YR, Leyton DL, Wells TJ, Wardius CA, Tveen-Jensen K, Morris FC, Knowles TJ, Cunningham AF, Cole JA, Henderson IR. A generalised module for the selective extracellular accumulation of recombinant proteins. *Microb Cell Fact*. 2012;11(1):69. doi:10.1186/1475-2859-11-69.
 26. Celik N, Webb CT, Leyton DL, Holt KE, Heinz E, Gorrell R, Kwok T, Naderer T, Strugnell RA, Speed TP, et al. A bioinformatic strategy for the detection, classification and analysis of bacterial autotransporters. *PLOS ONE*. 2012;7(8):e43245. doi:10.1371/journal.pone.0043245.
 27. Jong WSP, Schillemans M, Ten Hagen-Jongman CM, Luirink J, van Ulsen P. Comparing autotransporter β-domain configurations for their capacity to secrete heterologous proteins to the cell surface. *PLOS ONE*. 2018;13(2):e0191622. doi:10.1371/journal.pone.0191622.
 28. Drobnak I, Braselmann E, Chaney JL, Leyton DL, Bernstein HD, Lithgow T, Luirink J, Nataro JP, Clark PL. Of linkers and autochaperones: an unambiguous nomenclature to identify common and uncommon themes for autotransporter secretion. *Mol Microbiol*. 2015;95(1):1–16. doi:10.1111/mmi.12838.
 29. Velarde JJ, Nataro JP. Hydrophobic residues of the autotransporter EspP linker domain are important for outer membrane translocation of its passenger. *J Biol Chem*. 2004;279(30):31495–31504. doi:10.1074/jbc.M404424200.
 30. Doyle MT, Bernstein HD. BamA forms a translocation channel for polypeptide export across the bacterial outer membrane. *Mol Cell*. 2021;81(9):2000–12 e3. doi:10.1016/j.molcel.2021.02.023.
 31. Ieva R, Bernstein HD. Interaction of an autotransporter passenger domain with BamA during its translocation across the bacterial outer membrane. *Proc Natl Acad Sci USA*. 2009;106(45):19120–19125. doi:10.1073/pnas.0907912106.
 32. Jong WS, ten Hagen-Jongman CM, den Blaauwen T, Slotboom DJ, Tame JR, Wickstrom D, De Gier J-W, Otto BR, Luirink J. Limited tolerance towards folded elements during secretion of the autotransporter Hbp. *Mol Microbiol*. 2007;63(5):1524–1536. doi:10.1111/j.1365-2958.2007.05605.x.
 33. Dautin N. Folding control in the path of type 5 secretion. *Toxins (Basel)*. 2021;13(5):341. doi:10.3390/toxins13050341.

34. Stein M, Kenny B, Stein MA, Finlay BB. Characterization of EspC, a 110-kilodalton protein secreted by enteropathogenic *Escherichia coli* which is homologous to members of the immunoglobulin a protease-like family of secreted proteins. *J Bacteriol.* 1996;178(22):6546–6554. doi:10.1128/jb.178.22.6546-6554.1996.
35. Pokharel P, Habouria H, Bessaiah H, Dozois CM. Serine protease autotransporters of the Enterobacteriaceae (SPATEs): out and about and chopping it up. *Microorganisms.* 2019;7(12):594. doi:10.3390/microorganisms7120594.
36. Barnard TJ, Gumbart J, Peterson JH, Noinaj N, Easley NC, Dautin N, Kuszak AJ, Tajkhorshid E, Bernstein HD, Buchanan SK. Molecular basis for the activation of a catalytic asparagine residue in a self-cleaving bacterial autotransporter. *J Mol Biol.* 2012;415(1):128–142. doi:10.1016/j.jmb.2011.10.049.
37. Dautin N, Barnard TJ, Anderson DE, Bernstein HD. Cleavage of a bacterial autotransporter by an evolutionarily convergent autocatalytic mechanism. *Embo J.* 2007;26(7):1942–1952. doi:10.1038/sj.emboj.7601638.
38. Tajima N, Kawai F, Park SY, Tame JR. A novel intein-like autoproteolytic mechanism in autotransporter proteins. *J Mol Biol.* 2010;402(4):645–656. doi:10.1016/j.jmb.2010.06.068.
39. Snell LM, McGaha TL, Brooks DG. Type I interferon in chronic virus infection and cancer. *Trends Immunol.* 2017;38(8):542–557. doi:10.1016/j.it.2017.05.005.
40. Lazear HM, Schoggins JW, Diamond MS. Shared and distinct functions of type I and Type III interferons. *Immunity.* 2019;50(4):907–923. doi:10.1016/j.immuni.2019.03.025.
41. McNab F, Mayer-Barber K, Sher A, Wack A, O'Garra A. Type I interferons in infectious disease. *Nat Rev Immunol.* 2015;15(2):87–103. doi:10.1038/nri3787.
42. Gibbert K, Schlaak JF, Yang D, Dittmer U. IFN- α subtypes: distinct biological activities in anti-viral therapy. *Br J Pharmacol.* 2013;168(5):1048–1058. doi:10.1111/bph.12010.
43. Kalie E, Jaitin DA, Abramovich R, Schreiber G. An interferon $\alpha 2$ mutant optimized by phage display for IFNAR1 binding confers specifically enhanced antitumor activities. *J Biol Chem.* 2007;282(15):11602–11611. doi:10.1074/jbc.M610115200.
44. Jong WS, Sopova Z, de Punder K, ten Hagen-Jongman CM, Wagner S, Wickstrom D, de Gier J-W, Andersen P, van der Wel NN, Luirink J. A structurally informed autotransporter platform for efficient heterologous protein secretion and display. *Microb Cell Fact.* 2012;11(1):85. doi:10.1186/1475-2859-11-85.
45. Gratz A, Bollacke A, Stephan S, Nienberg C, Le Borgne M, Gotz C, Jose J. Functional display of heterotetrameric human protein kinase CK2 on *Escherichia coli*: a novel tool for drug discovery. *Microb Cell Fact.* 2015;14(1):74. doi:10.1186/s12934-015-0263-z.
46. Petrovskaya LE, Zlobin AV, Shingarova LN, Boldyreva EF, Gapizov SS, Novototskaya-Vlasova KA, Rivkina EM, Dolgikh DA, Kirpichnikov MP. Fusion with the cold-active esterase facilitates autotransporter-based surface display of the 10th human fibronectin domain in *Escherichia coli*. *Extremophiles.* 2018;22(1):141–150. doi:10.1007/s00792-017-0990-7.
47. Quehl P, Hollender J, Schuurmann J, Brossette T, Maas R, Jose J. Co-expression of active human cytochrome P450 1A2 and cytochrome P450 reductase on the cell surface of *Escherichia coli*. *Microb Cell Fact.* 2016;15(1):26. doi:10.1186/s12934-016-0427-5.
48. Iguchi A, Thomson NR, Ogura Y, Saunders D, Ooka T, Henderson IR, Harris D, Asadulghani M, Kurokawa K, Dean P, et al. Complete genome sequence and comparative genome analysis of enteropathogenic *Escherichia coli* O127: H6 strain E2348/69. *J Bacteriol.* 2009;191(1):347–354. doi:10.1128/JB.01238-08.
49. Shaulov L, Gershberg J, Deng W, Finlay BB, Sal-Man N, Roy CR, McDaniel LS. The ruler protein EscP of the enteropathogenic *Escherichia coli* type III secretion system is involved in calcium sensing and secretion hierarchy regulation by interacting with the gatekeeper protein SepL. *mBio.* 2017;8(1). doi:10.1128/mBio.01733-16.
50. Wilmaerts D, Dewachter L, De Loose PJ, Bollen C, Verstraeten N, Michiels J. HokB monomerization and membrane repolarization control persister awakening. *Mol Cell.* 2019;75(5):1031–42 e4. doi:10.1016/j.molcel.2019.06.015.
51. Edwards RA, Keller LH, Schifferli DM. Improved allelic exchange vectors and their use to analyze 987P fimbria gene expression. *Gene.* 1998;207(2):149–157. doi:10.1016/S0378-1119(97)00619-7.
52. Krasnopolsky S, Kuzmina A, Taube R, Bangham CRM. Genome-wide CRISPR knockout screen identifies ZNF304 as a silencer of HIV transcription that promotes viral latency. *PLOS Pathog.* 2020;16(9):e1008834. doi:10.1371/journal.ppat.1008834.
53. Gibson DG, Benders GA, Andrews-Pfannkoch C, Denisova EA, Baden-Tillson H, Zaveri J, Stockwell TB, Brownley A, Thomas DW, Algire MA, et al. Complete chemical synthesis, assembly, and cloning of a *Mycoplasma genitalium* genome. *Science.* 2008;319(5867):1215–1220. doi:10.1126/science.1151721.
54. Gibson DG, Young L, Chuang RY, Venter JC, Hutchison CA 3rd, Smith HO. Enzymatic assembly of DNA molecules up to several hundred kilobases. *Nat Methods.* 2009;6(5):343–345. doi:10.1038/nmeth.1318.
55. Tejeda-Dominguez F, Huerta-Cantillo J, Chavez-Duenas L, Navarro-Garcia F. A novel mechanism for protein delivery by the type 3 secretion system for extracellularly secreted proteins. *mBio.* 2017;8(2). doi:10.1128/mBio.00184-17.

56. Andersson KG, Persson J, Stahl S, Lofblom J. Autotransporter-mediated display of a naïve affibody library on the outer membrane of *Escherichia coli*. *Biotechnol J*. 2019;14(4):e1800359. doi:10.1002/biot.201800359.
57. Navarro-Garcia F, Serapio-Palacios A, Vidal JE, Salazar MI, Tapia-Pastrana G. EspC promotes epithelial cell detachment by enteropathogenic *Escherichia coli* via sequential cleavages of a cytoskeletal protein and then focal adhesion proteins. *Infect Immun*. 2014;82(6):2255–2265. doi:10.1128/IAI.01386-13.
58. Oliver DC, Huang G, Nodel E, Pleasance S, Fernandez RC. A conserved region within the *Bordetella pertussis* autotransporter BrkA is necessary for folding of its passenger domain. *Mol Microbiol*. 2003;47(5):1367–1383. doi:10.1046/j.1365-2958.2003.03377.x.
59. Peterson JH, Tian P, Ieva R, Dautin N, Bernstein HD. Secretion of a bacterial virulence factor is driven by the folding of a C-terminal segment. *Proc Natl Acad Sci USA*. 2010;107(41):17739–17744. doi:10.1073/pnas.1009491107.
60. Soprova Z, Sauri A, van Ulsen P, Tame JR, den Blaauwen T, Jong WS, Luirink J. A conserved aromatic residue in the autochaperone domain of the autotransporter Hbp is critical for initiation of outer membrane translocation. *J Biol Chem*. 2010;285(49):38224–38233. doi:10.1074/jbc.M110.180505.
61. Deng W, Li Y, Hardwidge PR, Frey EA, Pfuertner RA, Lee S, Gruenheid S, Strynacka NCJ, Puente JL, Finlay BB. Regulation of type III secretion hierarchy of translocators and effectors in attaching and effacing bacterial pathogens. *Infect Immun*. 2005;73(4):2135–2146. doi:10.1128/IAI.73.4.2135-2146.2005.
62. Elliott SJ, Sperandio V, Giron JA, Shin S, Mellies JL, Wainwright L, Hutcheson SW, McDaniel TK, Kaper JB. The locus of enterocyte effacement (LEE)-encoded regulator controls expression of both LEE- and non-lee-encoded virulence factors in enteropathogenic and enterohemorrhagic *Escherichia coli*. *Infect Immun*. 2000;68(11):6115–6126. doi:10.1128/IAI.68.11.6115-6126.2000.
63. Kenny B, Abe A, Stein M, Finlay BB. Enteropathogenic *Escherichia coli* protein secretion is induced in response to conditions similar to those in the gastrointestinal tract. *Infect Immun*. 1997;65(7):2606–2612. doi:10.1128/iai.65.7.2606-2612.1997.
64. Abadie V, Kim SM, Lejeune T, Palanski BA, Ernest JD, Tastet O, Voisine J, Discepolo V, Marietta EV, Hawash MBF, et al. IL-15, gluten and HLA-DQ8 drive tissue destruction in coeliac disease. *Nature*. 2020;578(7796):600–604. doi:10.1038/s41586-020-2003-8.
65. Leyton DL, Sevastyanovich YR, Browning DF, Rossiter AE, Wells TJ, Fitzpatrick RE, Overduin M, Cunningham AF, Henderson IR. Size and conformation limits to secretion of disulfide-bonded loops in autotransporter proteins. *J Biol Chem*. 2011;286(49):42283–42291. doi:10.1074/jbc.M111.306118.
66. Klaus W, Gsell B, Labhardt AM, Wipf B, Senn H. The three-dimensional high resolution structure of human interferon α -2a determined by heteronuclear NMR spectroscopy in solution. *J Mol Biol*. 1997;274(4):661–675. doi:10.1006/jmbi.1997.1396.
67. Bardwell JC, McGovern K, Beckwith J. Identification of a protein required for disulfide bond formation in vivo. *Cell*. 1991;67(3):581–589. doi:10.1016/0092-8674(91)90532-4.
68. Li Y, Batra S, Sassano A, Majchrzak B, Levy DE, Gaestel M, Fish EN, Davis RJ, Platanias LC. Activation of mitogen-activated protein kinase kinase (MKK) 3 and MKK6 by type I interferons. *J Biol Chem*. 2005;280(11):10001–10010. doi:10.1074/jbc.M410972200.
69. Van Winkle JA, Constant DA, Li L, Nice TJ. Selective interferon responses of intestinal epithelial cells minimize tumor necrosis factor α cytotoxicity. *J Virol*. 2020;94(21). doi:10.1128/JVI.00603-20.
70. Ciesielska A, Matyjek M, Kwiatkowska K. TLR4 and CD14 trafficking and its influence on LPS-induced pro-inflammatory signaling. *Cell Mol Life Sci*. 2021;78(4):1233–1261. doi:10.1007/s00018-020-03656-y.
71. Torkashvand F, Vaziri B. Main quality attributes of monoclonal antibodies and effect of cell culture components. *Iran Biomed J*. 2017;21(3):131–141. doi:10.18869/acadpub.ijb.21.3.131.
72. Goldring JP. Methods to concentrate proteins for protein isolation, proteomic, and peptidomic evaluation. *Methods Mol Biol*. 2015;1314:5–18.
73. Jaitin DA, Roisman LC, Jaks E, Gavutis M, Piehler J, Van der Heyden J, Uze G, Schreiber G. Inquiring into the differential action of interferons (IFNs): an IFN- α 2 mutant with enhanced affinity to IFNAR1 is functionally similar to IFN- β . *Mol Cell Biol*. 2006;26(5):1888–1897. doi:10.1128/MCB.26.5.1888-1897.2006.
74. Kalie E, Jaitin DA, Podoplelova Y, Piehler J, Schreiber G. The stability of the ternary interferon-receptor complex rather than the affinity to the individual subunits dictates differential biological activities. *J Biol Chem*. 2008;283(47):32925–32936. doi:10.1074/jbc.M806019200.
75. Quadat-Akabayov SR, Chill JH, Levy R, Kessler N, Anglistter J. Determination of the human type I interferon receptor binding site on human interferon- α 2 by cross saturation and an NMR-based model of the complex. *Protein Sci*. 2006;15(11):2656–2668. doi:10.1110/ps.062283006.
76. Harari D, Abramovich R, Zozulya A, Smith P, Pouly S, Koster M, Hauser H, Schreiber G. Bridging the species divide: transgenic mice humanized for type-I interferon response. *PLOS ONE*. 2014;9(1):e84259. doi:10.1371/journal.pone.0084259.